NASA/TM—2002-211566

Thin Film Heat Flux Sensor of Improved Design

Gus Fralick and John Wrbanek
Glenn Research Center, Cleveland, Ohio

Charles Blaha
Akima Corporation, Cleveland, Ohio

September 2002

The NASA STI Program Office . . . in Profile

Since its founding, NASA has been dedicated to the advancement of aeronautics and space science. The NASA Scientific and Technical Information (STI) Program Office plays a key part in helping NASA maintain this important role.

The NASA STI Program Office is operated by Langley Research Center, the Lead Center for NASA's scientific and technical information. The NASA STI Program Office provides access to the NASA STI Database, the largest collection of aeronautical and space science STI in the world. The Program Office is also NASA's institutional mechanism for disseminating the results of its research and development activities. These results are published by NASA in the NASA STI Report Series, which includes the following report types:

- TECHNICAL PUBLICATION. Reports of completed research or a major significant phase of research that present the results of NASA programs and include extensive data or theoretical analysis. Includes compilations of significant scientific and technical data and information deemed to be of continuing reference value. NASA's counterpart of peer-reviewed formal professional papers but has less stringent limitations on manuscript length and extent of graphic presentations.
- TECHNICAL MEMORANDUM. Scientific and technical findings that are preliminary or of specialized interest, e.g., quick release reports, working papers, and bibliographies that contain minimal annotation. Does not contain extensive analysis.
- CONTRACTOR REPORT. Scientific and technical findings by NASA-sponsored contractors and grantees.
- CONFERENCE PUBLICATION. Collected papers from scientific and technical conferences, symposia, seminars, or other meetings sponsored or cosponsored by NASA.
- SPECIAL PUBLICATION. Scientific, technical, or historical information from NASA programs, projects, and missions, often concerned with subjects having substantial public interest.
- TECHNICAL TRANSLATION. English-language translations of foreign scientific and technical material pertinent to NASA's mission.

Specialized services that complement the STI Program Office's diverse offerings include creating custom thesauri, building customized databases, organizing and publishing research results . . . even providing videos.

For more information about the NASA STI Program Office, see the following:

- Access the NASA STI Program Home Page at ***http://www.sti.nasa.gov***
- E-mail your question via the Internet to help@sti.nasa.gov
- Fax your question to the NASA Access Help Desk at 301–621–0134
- Telephone the NASA Access Help Desk at 301–621–0390
- Write to:
  NASA Access Help Desk
  NASA Center for AeroSpace Information
  7121 Standard Drive
  Hanover, MD 21076

NASA/TM—2002-211566

Thin Film Heat Flux Sensor of Improved Design

Gus Fralick and John Wrbanek
Glenn Research Center, Cleveland, Ohio

Charles Blaha
Akima Corporation, Cleveland, Ohio

Prepared for the
48th International Instrumentation Symposium
sponsored by the Instrumentation, Systems, and Automation Society
San Diego, California, May 5–9, 2002

National Aeronautics and
Space Administration

Glenn Research Center

September 2002

This report contains preliminary findings, subject to revision as analysis proceeds.

The Aerospace Propulsion and Power Program at NASA Glenn Research Center sponsored this work.

Available from

NASA Center for Aerospace Information
7121 Standard Drive
Hanover, MD 21076

National Technical Information Service
5285 Port Royal Road
Springfield, VA 22100

Available electronically at http://gltrs.grc.nasa.gov

Thin Film Heat Flux Sensor of Improved Design

Gus Fralick and John Wrbanek
National Aeronautics and Space Administration
Glenn Research Center
Cleveland, Ohio

Charles Blaha
Akima Corporation
Cleveland, Ohio

ABSTRACT

A new design for a thin film heat flux sensor is presented. It is easier to fabricate than previous designs, for a given heat flux has an order of magnitude larger signal, and is more easily scalable than previous designs. Transient and steady state data are also presented.

INTRODUCTION

Heat flux is one of a number of parameters, together with pressure, temperature, flow, etc., of interest to engine designers and fluid dynamicists. There are various designs of heat flux sensors, such as Gardon gauges (Ref. 1), plug gauges (Ref. 2), and thin film thermocouple arrays (Ref. 3). The thin film types have the advantage of high frequency response and minimal flow disturbance (Ref. 4).

All heat flux sensors operate by measuring the temperature difference across a thermal resistance. Current designs use thermocouples to measure this temperature difference. Because of the small temperature differences involved, and the small output of a single junction, the thermocouples are arranged as a thermopile (Fig. 1). This raises the output by a factor of 30 to 100, depending on the number of junctions in the array. Nevertheless, the signal level is still low, typically a few $\mu V/(Watt/cm^2)$. In addition, the precise alignment required to place each thermocouple element correctly makes fabrication difficult, and restricts the minimum size to about a fourth of an inch in diameter.

Thus we seek a design that retains the advantages of thin films, has a larger output, is easier to fabricate, and can be made smaller.

FABRICATION

The new sensor design consists of a Wheatstone bridge deposited onto a 0.040 in. (1 mm) alumina substrate. Since one is fabricating a resistor array rather than a thermocouple array, this design is much simpler to fabricate than other designs. Alumina is chosen because its thermal conductivity is relatively high (higher than some metals) so that the sensor will not change the thermal resistance and thus distort the measurement. Alumina also has good high temperature properties, and is inexpensive.

The temperature sensitive element is sputter deposited platinum, with line width and line spacing typically a few thousandths of an inch. Platinum also has excellent high temperature properties, and the variation of its electrical resistance with temperature is well characterized. The alumina is washed with soap and DI water, solvent cleaned, dried, and then the pattern applied using a newly developed photolithography technique. On the single sided gauges, approximately 5μm of silicon dioxide is sputtered over diagonally opposite arms of the bridge.

DESCRIPTION, PRINCIPLE OF OPERATION

Several variations of the new heat flux sensor are shown in figures 2 and 3, in both single sided and double-sided designs. In all cases, the sensor consists of a four active arm Wheatstone bridge, two arms of which are covered by an extra thermal resistance. In the two-sided designs, the substrate upon which the sensor is mounted acts as the extra resistance, and in the one sided designs, the extra resistance is sputtered or electron beam deposited over two of the arms. The bridge itself is made of a material with a high temperature coefficient of resistance, such as platinum or nickel.

With no heat flux applied to the sensor, all of the bridge elements (A, B, C and D in figures 2 and 3) are at the initial temperature $\mathbf{T_0}$, and have resistance $\mathbf{R_0}$. With the application of heat flux, the two elements of the bridge not covered by the layer of thermal resistance (B and C) are at a surface temperature designated $\mathbf{T_S}$, and the other two elements under the film of thermal resistance (A and D) are at the temperature $\mathbf{T_F < T_S}$. The resistance of the elements are then respectively $\mathbf{R_0[1+\beta(T_S-T_0)]}$ and $\mathbf{R_0[1+\beta(T_F-T_0)]}$, where β is the linear temperature coefficient of resistance.

If the bridge excitation is **V** volts, the output from one arm is

$$\mathbf{V_2 = V\frac{R_0\left[1+\beta(T_S-T_0)\right]}{R_0\left[1+\beta(T_S-T_0)\right]+R_0\left[1+\beta(T_F-T_0)\right]}}$$

and from the other arm is

$$\mathbf{V_1 = V\frac{R_0\left[1+\beta(T_F-T_0)\right]}{R_0\left[1+\beta(T_S-T_0)\right]+R_0\left[1+\beta(T_F-T_0)\right]}}.$$

Notice that, $\mathbf{R_0}$, the initial value of the resistance, cancels.

The instantaneous output from the sensor is then

$$\mathbf{V_{SIG} = V_2 - V_1 = V\frac{\beta(T_S-T_F)}{2+\beta\left[(T_F-T_0)+(T_S-T_0)\right]}}.$$

Modeling the gauge then consists of calculating the values of $\mathbf{T_F}$ and $\mathbf{T_S}$ and relating them to the incident heat flux.

STEADY STATE RESPONSE

The gauge is modeled as one-dimensional heat transfer into a two-layer composite as shown in figure 4. The gauge, of thickness **l**, is mounted on a heat sink, of thickness **L**. The interface between the layers is at $\mathbf{x = 0}$, the surface exposed to the heat flux **Q** is at $\mathbf{x = -l}$, and the base of the substrate is at $\mathbf{x = L}$. In the region $\mathbf{-l<x<0}$, the temperature is $\mathbf{T_1\ (x)}$, and the thermal conductivity is $\mathbf{k_1}$. In the region **0<x<L**, the temperature is $\mathbf{T_2}$ **(x)**, and the thermal conductivity is $\mathbf{k_2}$. The temperatures $\mathbf{T_1}$ and $\mathbf{T_2}$ satisfy the steady state heat equation $\frac{d^2T}{dx^2} = 0$, and satisfy the boundary conditions

$$-k_1 \frac{dT_1}{dx}(x = -l) = Q$$

$$T_1(0) = T_2(0)$$

$$k_1 \frac{dT_1}{dx}(0) = k_2 \frac{dT_2}{dx}(0)$$

$$T_2(x = L) = T_0$$

The solution is $T_1(x) = -Q\frac{x}{k_1} + Q\frac{L}{k_2} + T_0$, $T_2(x) = Q\frac{(L-x)}{k_2} + T_0$, so that $T_S = T_1(x = -l) = Q\left(\frac{l}{k_1} + \frac{L}{k_2}\right) + T_0$, $T_F = T(0) = Q\frac{L}{k_2} + T_0$, $T_S - T_F = Q\frac{l}{k_1}$, and for steady state heat flux, the sensor output is

$$V_{SIG} = \frac{V\beta Q\frac{l}{k_1}}{2 + \beta Q\left(\frac{l}{k_1} + 2\frac{L}{k_2}\right)}.$$

Typically, for the two sided gauge,

l = 0.040" = 1.016 x 10^{-3} m
L = 1" = 2.54 x 10^{-2} m
$\mathbf{k_1}$ = 36 W/m/K (Al_2O_3)
$\mathbf{k_2}$ = 15 W/m/K (type 304 stainless)
β = 3.98 x 10^{-3} K^{-1} (Pt).

With a bridge excitation **V** of one volt and a heat flux **Q** of 1 W/cm^2 = 10^4 W/m^2,

$$V_{SIG} = \frac{1.13\text{x}10^{-3}}{2.137} = 528\ (\mu V/V)/(W/cm^2).$$

For the one sided gauge, one would typically sputter approximately 5µm SiO_2 ($\mathbf{k_1}$ = 1.4 W/m/K) over the appropriate arms of the bridge. In this case, the output is approximately 68 (µV/V)/(W/cm^2). These outputs compare favorably with values for commercial gauges, 150 µV/(W/cm^2) and 8 µV/(W/cm^2) for high temperature gauges.

TRANSIENT RESPONSE

In many applications, the transient response of the gauge is of interest. For time varying heat flux, or while the gauge is coming to equilibrium, it is necessary to find $\mathbf{T_S}$ and $\mathbf{T_F}$ as functions of time. The temperatures in each layer, the gauge and the substrate, satisfy the heat equation

$$\rho c \frac{\partial T}{\partial t} = k \frac{\partial^2 T}{\partial x^2},$$

where ρ = mass density, kg/m^3
$\mathbf{c}$ = specific heat, J/kg/K
and $\mathbf{k}$ = thermal conductivity, W/m/K.

For a semi-infinite plane initially at temperature $\mathbf{T_0}$, with a constant heat flux $\mathbf{Q}$ into the surface at $\mathbf{x=0}$, starting at $\mathbf{t = 0}$, the temperature as a function of $\mathbf{x}$ and $\mathbf{t}$ is

$$T(x,t) - T_0 = \frac{2Q}{k}\sqrt{\frac{\alpha t}{\pi}}\, e^{-\frac{x^2}{4\alpha t}} - \frac{Qx}{k}\operatorname{erfc}\left(\frac{x}{2\sqrt{\alpha t}}\right)$$

where $\alpha = \dfrac{k}{\rho c}$ is the thermal diffusivity, m^2/s,

and $\operatorname{erfc}(x) = 1 - \operatorname{erf}(x) = 1 - \dfrac{2}{\sqrt{\pi}}\displaystyle\int_0^x e^{-t^2}dt$ is the complementary error function. Note that $\mathbf{erfc(0) = 1}$, and $\mathbf{erfc(\infty) = 0}$. (Ref. 5)

Laplace Transforms can be used to find solutions in terms of infinite series of error functions for the case of planes of finite thickness and for composite planes, but a more practical approach is to solve the problem numerically. In addition, it is possible to solve such problems as temperature dependant material properties or time varying heat flux.

A one dimensional finite volume technique (Ref. 6) was used to find the surface and film temperatures as function of time and position. At the surface $\mathbf{x = 0}$, a constant heat flux is applied starting at $\mathbf{t = 0}$, while at the other surface, $\mathbf{x = L}$, the temperature is held constant. The model is a layer of either 0.040 in. (1 mm) alumina for the two sided design or 5µm SiO_2 for the one sided design, on 1” (25.4 mm) stainless steel. The time variation is calculated fully implicitly. The temperatures $\mathbf{T_s}$ and $\mathbf{T_F}$ are respectively the calculated surface ($\mathbf{x = 0}$) and interface temperatures.

DISCUSSION

As can be seen from figures 5–8, the gauges exhibit first order response, with the double-sided gauge having a time constant of approximately 270 µsec and the single sided gauge a time constant of roughly 7 µsec. These correspond to frequency responses (-3dB) of about 589 Hz and 23 kHz, respectively. The response of the single sided gauge is comparable to that of the fastest commercial gauges, with advertised time constants of 6±2 µsec.

Although testing the sensors in relevant environments is planned, experimentally verifying these numbers is problematical. As it is difficult to produce a step change in heat flux, it may be necessary to use the procedure used in ref. 4 to measure frequency response, that is, to chop the beam from a high power laser to produce a square wave input to the gauge, measure the rate at which the harmonics of the output signal decay with frequency, and compare the decay rate with that of an ideal system with an infinite frequency response. A thermopile design that should have dynamics similar to our single sided design showed a frequency response of only a few kHz. This may be because the insulator used in the thermopile design was nearly transparent to the laser light, lessening the temperature difference, and producing a "droopy" square wave and lower amplitude harmonics. The large amount of metal in the thermopile also reduces the temperature difference. It may also be possible to test gauge response by using a shock tube, but the heat transfer coefficient is unknown. At this point, numerical simulation may be the best option, at least for comparing designs.

CONCLUSION

We have described in this paper a thin film heat flux sensor that is simpler to fabricate than previous gauges, has higher output, and excellent transient response.

Construction of the double sided and single sided designs is ongoing, and in the near future we will be able to compare the predicted and actual gauge outputs.

REFERENCES

1. R. Gardon, An Instrument for the Direct Measurement of Intense Thermal Radiation, *Review of Scientific Measurements*, 24, 5, 1953, pp. 366–370.
2. C.H. Liebert, "Miniature High Temperature Plug-Type Heat Flux Gages", NASA TM–105403, April 1992.
3. H. Will, "Fabrication of Thin Film Heat Flux Sensors", *Proceedings of the Third Health Monitoring Conference for Space Propulsion Systems,* University of Cincinnati Press, Cincinnati, OH, 1991, pp. 348–355.
4. C.S. Cho, G.C. Fralick, and H.D. Bhatt, "Steady State and Frequency Response of a Thin Film Heat Flux Gauge", *Journal of Spacecraft and Rockets*, 34, 6, 1997, pp. 792–798.
5. F.D. Incropera and D.P. DeWitt, *Fundamentals of Heat and Mass Transfer*, 3rd edition, Wiley and Sons, New York, 1990.
6. D.A. Anderson, J.C. Tannehill, and R.H. Pletcher, *Computational Fluid Mechanics and Heat Transfer,* Hemisphere Publishing Corp., Washington, 1984.

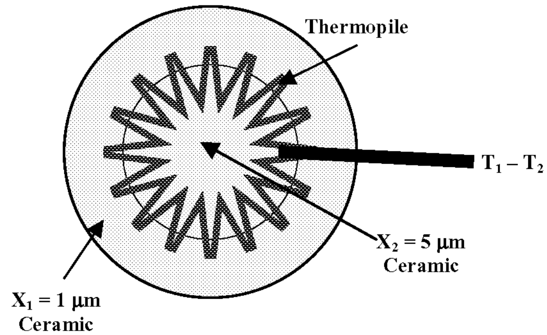

Figure 1: Thermopile-Based Thin Film Heat Flux Sensor (Heat Flux is into the picture).

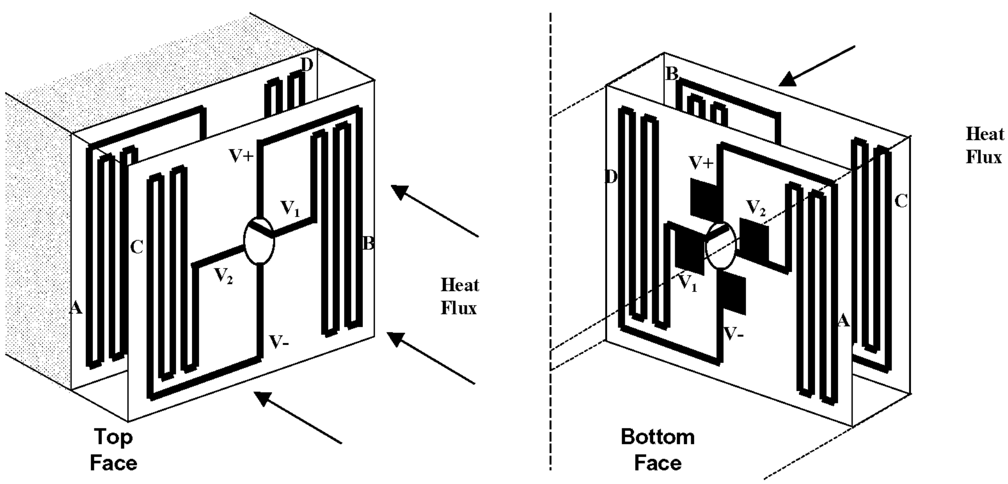

Figure 2: Double-Sided Thin Film Wheatstone Bridge Heat Flux Sensor.

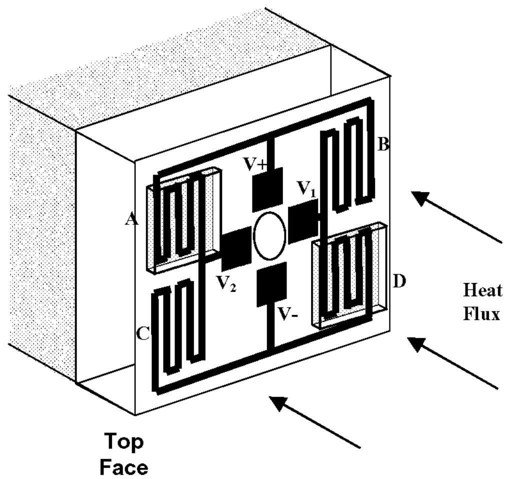

Figure 3: Single-Sided Thin Film Wheatstone Bridge Heat Flux Sensor.

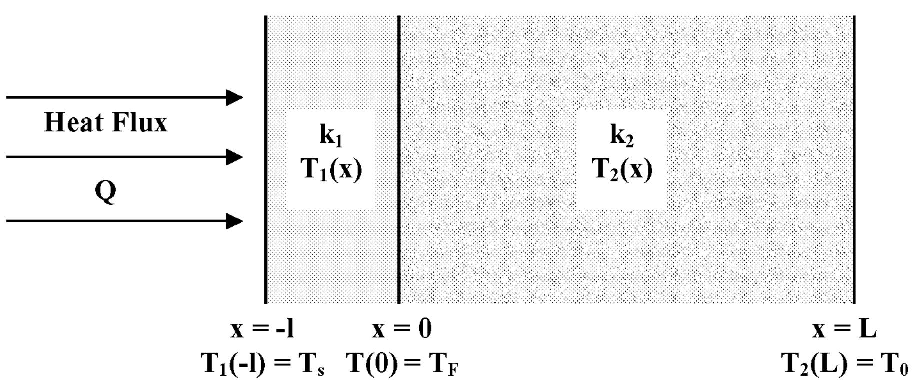

Figure 4: Schematic of One-Dimensional Heat Transfer into a Two-Layer Composite.

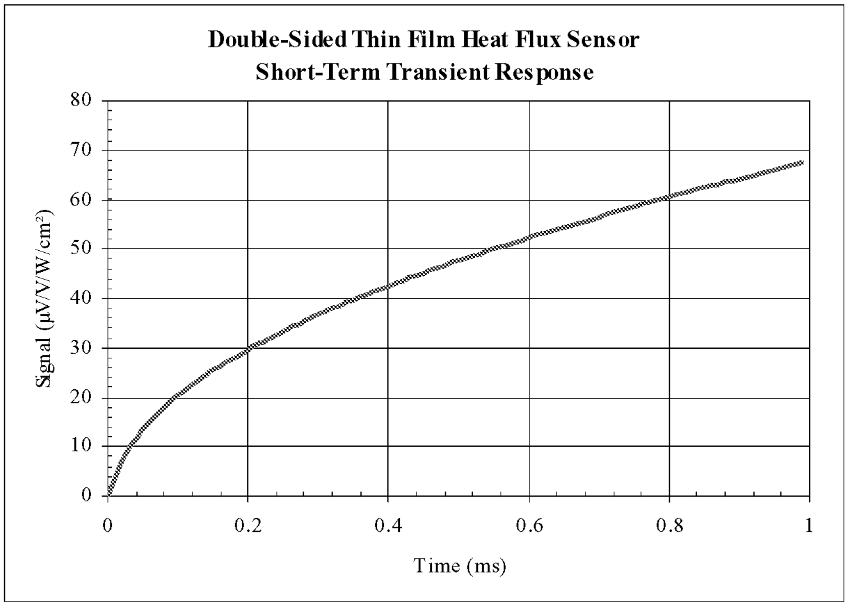

Figure 5: Modeled Short-Term Response for a Double-Sided Wheatstone Bridge Heat Flux Sensor.

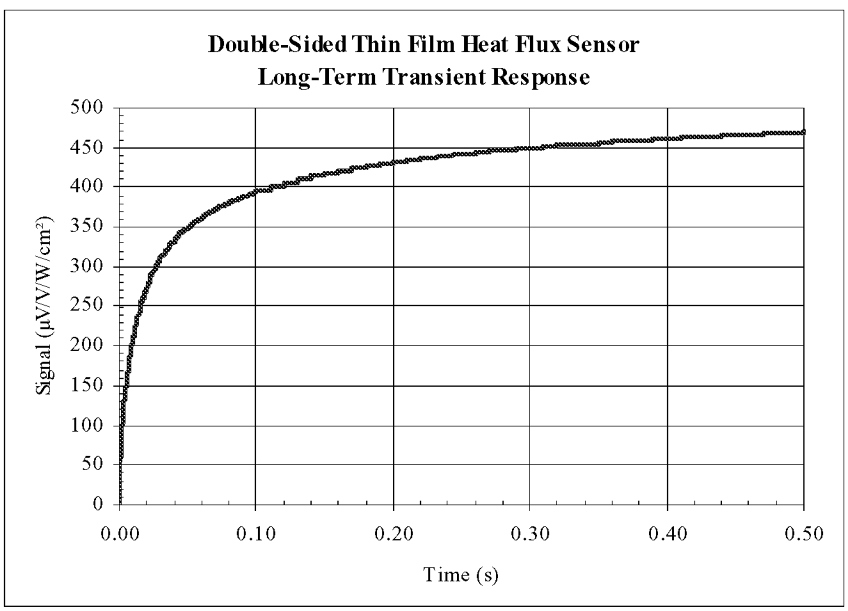

Figure 6: Modeled Long-Term Response for a Double-Sided Wheatstone Bridge Heat Flux Sensor.

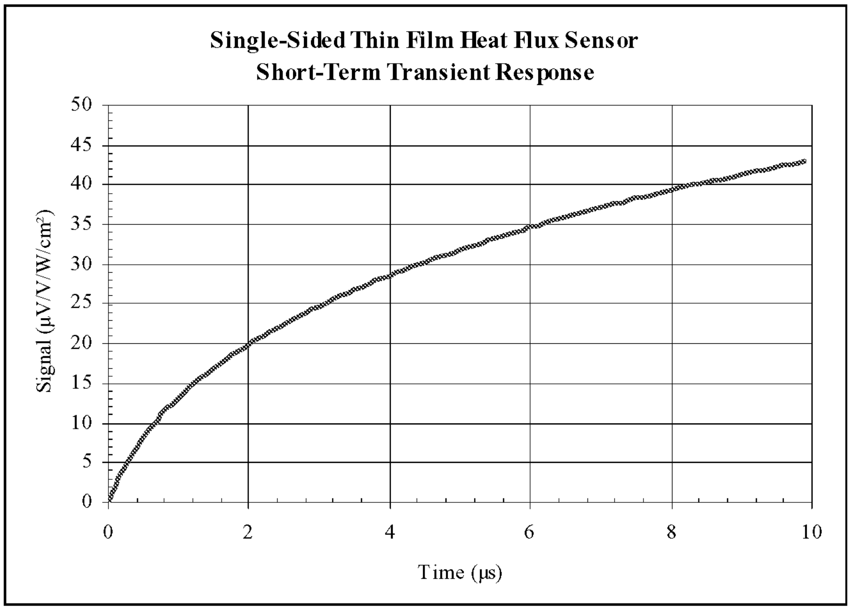

Figure 7: Modeled Short-Term Response for a Single-Sided Wheatstone Bridge Heat Flux Sensor.

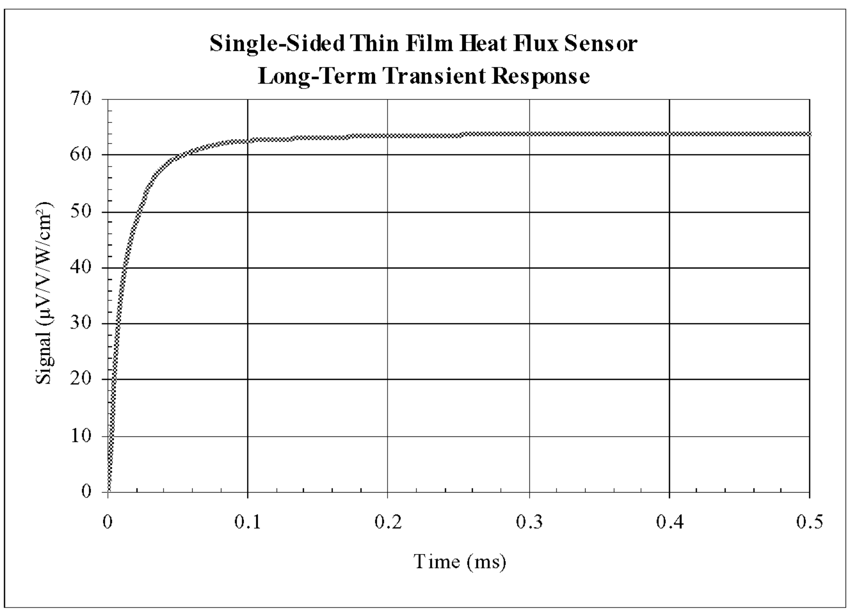

Figure 8: Modeled Long-Term Response for a Single-Sided Wheatstone Bridge Heat Flux Sensor.

REPORT DOCUMENTATION PAGE

Form Approved
OMB No. 0704-0188

1. AGENCY USE ONLY (*Leave blank*)	2. REPORT DATE	3. REPORT TYPE AND DATES COVERED
	September 2002	Technical Memorandum

4. TITLE AND SUBTITLE

Thin Film Heat Flux Sensor of Improved Design

5. FUNDING NUMBERS

WU–708–48–13–00

6. AUTHOR(S)

Gus Fralick, John Wrbanek, and Charles Blaha

7. PERFORMING ORGANIZATION NAME(S) AND ADDRESS(ES)

National Aeronautics and Space Administration
John H. Glenn Research Center at Lewis Field
Cleveland, Ohio 44135–3191

8. PERFORMING ORGANIZATION REPORT NUMBER

E–13350

9. SPONSORING/MONITORING AGENCY NAME(S) AND ADDRESS(ES)

National Aeronautics and Space Administration
Washington, DC 20546–0001

10. SPONSORING/MONITORING AGENCY REPORT NUMBER

NASA TM—2002-211566

11. SUPPLEMENTARY NOTES

Prepared for the 48th International Instrumentation Symposium sponsored by the Instrumentation, Systems, and Automation Society, San Diego, California, May 5–9, 2002. Gus Fralick and John Wrbanek, NASA Glenn Research Center; and Charles Blaha, Akima Corporation, Cleveland, Ohio 44135. Responsible person, Gus Fralick, organization code 5510, 216–433–3645.

12a. DISTRIBUTION/AVAILABILITY STATEMENT

Unclassified - Unlimited
Subject Category: 35 Distribution: Nonstandard

Available electronically at http://gltrs.grc.nasa.gov

This publication is available from the NASA Center for AeroSpace Information, 301–621–0390.

12b. DISTRIBUTION CODE

13. ABSTRACT ***(Maximum 200 words)***

A new design for a thin film heat flux sensor is presented. It is easier to fabricate than previous designs, for a given heat flux has an order of magnitude larger signal, and is more easily scalable than previous designs. Transient and steady state data are also presented.

14. SUBJECT TERMS

Heat flux; Thin film sensor

15. NUMBER OF PAGES

15

16. PRICE CODE

17. SECURITY CLASSIFICATION OF REPORT	18. SECURITY CLASSIFICATION OF THIS PAGE	19. SECURITY CLASSIFICATION OF ABSTRACT	20. LIMITATION OF ABSTRACT
Unclassified	Unclassified	Unclassified	